

Large-Angle Correlations in the Cosmic Microwave Background

George Efstathiou, Yin-Zhe Ma and Duncan Hanson

Kavli Institute for Cosmology Cambridge and Institute of Astronomy, Madingley Road, Cambridge, CB3 0HA.

6 November 2018

ABSTRACT

It has been argued recently by Copi *et al.* (2009) that the lack of large angular correlations of the CMB temperature field provides strong evidence against the standard, statistically isotropic, inflationary Λ CDM cosmology. We compare various estimators of the temperature correlation function showing how they depend on assumptions of statistical isotropy and how they perform on the WMAP 5 year ILC maps with and without a sky cut. We show that the low multipole harmonics that determine the large-scale features of the temperature correlation function can be reconstructed accurately, independent of any assumptions concerning statistical isotropy, from the data that lie outside the sky cuts. The temperature correlation functions computed from our reconstructions are in good agreement with those computed from the whole sky. A Bayesian analysis of the large-scale correlations is presented which shows that the data cannot exclude the standard Λ CDM model. We discuss the differences between our conclusions and those of Copi *et al.*

Key words: Methods: data analysis, statistical; Cosmology: cosmic microwave background, large-scale structure of Universe

1 INTRODUCTION

Following the discovery by the COBE team of temperature anisotropies in the cosmic microwave background (CMB) radiation (Smoot *et al.* 1992; Wright *et al.* 1992), Hinshaw *et al.* (1996) noticed that the temperature angular correlation function, $C(\theta)$, measured from the COBE maps was close to zero on large angular scales. This result attracted little attention until the publication of the first year results from WMAP (Bennett *et al.* 2003; Spergel *et al.* 2003, hereafter S03). The results from WMAP confirmed the lack of large-scale angular correlations in the temperature maps and led S03 to introduce the statistic

$$S_{1/2} = \int_{-1}^{1/2} [C(\theta)]^2 d \cos \theta. \quad (1)$$

The form of the statistic and the upper cut-off, $\mu = \cos \theta = 1/2$, were chosen *a posteriori* by S03 ‘in response’ to the observed shape of the temperature correlation function computed using a particular estimator and sky cut (as described in further detail in Section 2). To assess the statistical significance of the lack of large-scale power, S03 computed a ‘p-value’, *i.e.* the fraction of models in their Monte Carlo Markov chains which had a value of $S_{1/2}^{\text{model}} < S_{1/2}^{\text{data}}$, using the same estimator and sky cut that they applied to the data. For their standard six-parameter inflationary Λ CDM cosmology, they found a p-value of 0.15%, suggesting a significant discrepancy between the model and the data.

This problem was revisited by Efstathiou (2004a, hereafter E04). The main focus of the E04 paper was to improve on the pseudo-harmonic power spectrum analysis used by the WMAP team (Hinshaw *et al.* 2003) by using quadratic maximum likelihood (QML) estimates of the power spectrum, with particular emphasis on the statistical significance of the low amplitude of the quadrupole anisotropy. As an aside, E04 computed angular correlation functions from the QML power spectrum estimates and showed that they were insensitive to the presence of a sky cut. Similarly the $S_{1/2}$ statistic computed from these correlation functions was found to be insensitive to the size of the sky cut giving p-values of a few percent. E04 concluded that the correlation function and $S_{1/2}$ statistic offered no compelling evidence against the concordance inflationary Λ CDM model. E04 did not explore in any detail the low p-value for the $S_{1/2}$ statistic reported by S03 (2003), but commented that it

was probably simply an ‘unfortunate’ consequence of the particular choice of statistic, estimator and sky cut chosen by these authors (in other words, a result of various *a posteriori* choices).

The CMB temperature correlation function and S statistic have been reanalysed in two recent papers (Copi *et al.* 2007; Copi *et al.* 2009, hereafter CHSS09). The arguments in the two papers are quite similar, and so for the most part we will refer to the later paper (since, as in this work, it analyses the 5 year WMAP temperature data, Hinshaw *et al.* 2009). The Copi *et al.* papers are largely motivated by evidence for a violation of statistical isotropy in the WMAP temperature maps, in particular evidence of alignments amongst the low order CMB multipoles (*e.g.* Tegmark, de Oliveira-Costa and Hamilton 2003; Schwarz *et al.* 2004; Land and Magueijo 2005a, b), although the statistical significance of these alignments has been questioned (de Oliveira-Costa *et al.* 2004; Francis & Peacock 2009). Copi *et al.* make the valid point that statistical isotropy is often implicitly assumed in defining what is meant by the term ‘correlation function’ and in defining estimators. They argue further that different estimators contain different information. They then focus on pixel-based estimates of the correlation function applied to the WMAP data, including a sky cut, and find p-values for the $S_{1/2}$ statistic of ~ 0.025 – 0.04% , depending on the choice of CMB map and sky cut. If no sky cut is applied, they find p-values of $\sim 5\%$ (similar to the p-values reported in E04). CHSS09 comment that the full-sky results are apparently inconsistent with the cut-sky analysis suggesting a violation of statistical isotropy.

Any analysis which claims to strongly rule out the simple inflationary Λ CDM model deserves careful scrutiny, since a confirmed discordance would have profound consequences for our understanding of the early Universe. The purpose of this paper is to investigate carefully the analysis presented in CHSS09. In Section 2 we discuss estimators of the correlation function and relate the pixel-based estimator used by CHSS09 to the pseudo-power spectrum computed on a cut sky. In Section 3, we explicitly reconstruct the individual low order multipole coefficients $a_{\ell m}$ from cut-sky maps using a technique first applied by de Oliveira-Costa and Tegmark (2006). This allows us to test the sensitivity of the large-angle correlation function to the presence of a sky cut, independent of any assumptions concerning statistical isotropy or Gaussianity. The results of this analysis are compared with the QML estimates of the correlation function used in E04. Section 4 describes a Bayesian analysis of the $S_{1/2}$ statistic and contrasts it with the frequentist analysis applied by S03 and CHSS09. Our conclusions are summarized in Section 5.

2 ESTIMATORS OF THE CORRELATION FUNCTION

If we assume statistical isotropy, the ensemble average of the temperature angular correlation function (ACF) measured over the whole sky $\langle C(\theta) \rangle$ is related to the ensemble average of the angular power spectrum $\langle C_\ell \rangle$ by the well known relation

$$\langle C(\theta) \rangle = \frac{1}{4\pi} \sum_{\ell} (2\ell + 1) \langle C_\ell \rangle P_\ell(\cos \theta). \quad (2)$$

However, we have only one realization of the sky and we may further choose to impose a sky cut to reduce possible contamination from regions of high Galactic emission. If we relax the assumptions of statistical isotropy and complete sky coverage, there is no unique definition or estimator of the ACF. One can write down a number of estimators that, given certain assumptions concerning the underlying statistics of the fluctuations, may average to the ensemble mean when applied to data on an incomplete sky.

CHSS09 use a direct pixel based correlation function^{*} on the cut sky

$$C^{\text{pix}}(\theta) = \langle x_i x_j \rangle, \quad (3)$$

where x_i denotes the temperature value in pixel i and the angular brackets denote an average over all pixel pairs outside the sky cut with an angular separation that lies within a small interval of θ .

If the underlying temperature field is statistically isotropic, equation (3) provides an unbiased estimate of the correlation function, i.e. the average over a large number of independent realizations is unbiased, irrespective of the sky cut. However, if the fluctuations are statistically isotropic and Gaussian, (3) is not an optimal estimator of $\langle C(\theta) \rangle$. To see this, expand the temperature field in spherical harmonics

$$x_i = \sum_{\ell m} a_{\ell m} Y_{\ell m}(\boldsymbol{\theta}_i), \quad \langle |a_{\ell m}|^2 \rangle = \langle C_\ell \rangle. \quad (4)$$

Then, from the rotation properties of the spherical harmonics, it is straightforward to prove

$$C^{\text{pix}}(\theta_{ij}) = \langle x_i x_j \rangle = \frac{\sum_{\ell} (2\ell + 1) \tilde{C}_\ell^P P_\ell(\cos \theta_{ij})}{\sum_{\ell} (2\ell + 1) \tilde{W}_\ell P_\ell(\cos \theta_{ij})}, \quad (5)$$

^{*} More generally, one can define a bi-polar correlation function $C(\boldsymbol{\theta}_i, \boldsymbol{\theta}_j)$, which can be used as a test of statistical isotropy (see *e.g.* Basak, Hajian and Souradeep (2006)).

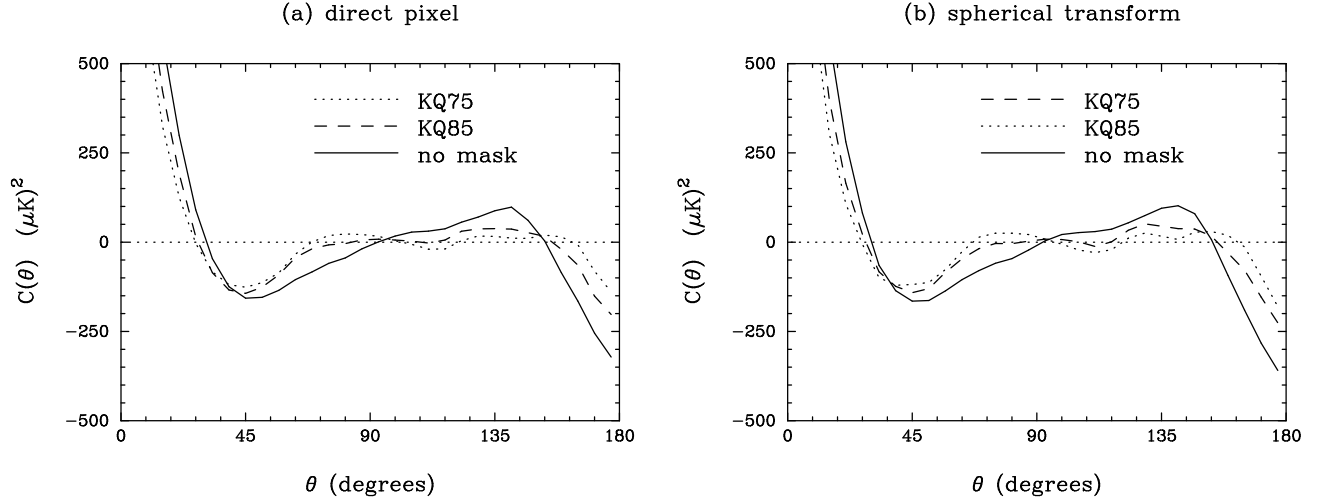


Figure 1. The figure to the left shows the correlation functions computed using the pixel estimator (3) applied to the 5 year WMAP ILC map (degraded as described in the text) over the full sky and with the WMAP KQ85 and KQ75 masks imposed. The figure to the right shows the correlation functions computed from the pseudo-power spectra (5).

where \tilde{C}_ℓ^P is the pseudo-power spectrum (PCL) estimate on the cut sky:

$$\tilde{C}_\ell^P = \frac{1}{(2\ell+1)} \sum_m |\tilde{a}_{\ell m}|^2, \quad \tilde{a}_{\ell m} = \sum_i x_i w_i Y_{\ell m}^*(\theta_i) \Omega_i, \quad (6)$$

where w_i is a window function that is zero or unity depending on whether a pixel (of area Ω_i) lies inside or outside the sky cut. The function \tilde{W}_ℓ in (5) is the pseudo-power spectrum of the window function w_i :

$$\tilde{W}_\ell = \frac{1}{(2\ell+1)} \sum_m |\tilde{w}_{\ell m}|^2, \quad \tilde{w}_{\ell m} = \sum_i w_i \Omega_i Y_{\ell m}^*(\theta_i). \quad (7)$$

The coefficients $\tilde{a}_{\ell m}$ are related to the coefficients $a_{\ell m}$ on the uncut sky by the coupling matrix \mathbf{K} ,

$$\tilde{a}_{\ell m} = \sum_{\ell' m'} a_{\ell' m'} K_{\ell m \ell' m'}, \quad (8)$$

where

$$K_{\ell_1 m_1 \ell_2 m_2} = \sum_i w_i \Omega_i Y_{\ell_1 m_1}^*(\theta_i) Y_{\ell_2 m_2}(\theta_i). \quad (9)$$

The relation (5) is an identity and does not depend on the assumption of statistical isotropy.

Under the assumption of statistical isotropy and Gaussianity, it is straightforward to calculate the covariance matrix of the estimator (3)

$$\langle \Delta \tilde{C}(\theta_i) \Delta \tilde{C}(\theta_j) \rangle = \left(\sum_{\ell_1 \ell_2} (2\ell_1+1)(2\ell_2+1) \langle \tilde{\Delta} C_{\ell_1}^P \tilde{\Delta} C_{\ell_2}^P \rangle P_{\ell_1}(\cos \theta_{ij}) P_{\ell_2}(\cos \theta_{ij}) \right) / \left(\sum_{\ell} (2\ell+1) \tilde{W}_\ell P_\ell(\cos \theta_{ij}) \right)^2 \quad (10)$$

where

$$\langle \Delta \tilde{C}_\ell^P \Delta \tilde{C}_{\ell'}^P \rangle = \frac{2}{(2\ell+1)(2\ell'+1)} \sum_{mm'} \sum_{\ell_1 m_1} \sum_{\ell_2 m_2} C_{\ell_1} C_{\ell_2} K_{\ell m \ell_1 m_1} K_{\ell' m' \ell_1 m_1}^* K_{\ell m \ell_2 m_2} K_{\ell' m' \ell_2 m_2}^* \quad (11)$$

Figure 1(a) shows the direct pixel based estimator (3) applied to the 5 year WMAP ILC map after smoothing with a Gaussian filter of 10° FWHM and repixelising at a Healpix (Gorski *et al.*, 2005) resolution NSIDE=16. The results of Figure 1 are consistent with those of CHSS09. With the WMAP KQ85 and KQ75 masks[†] applied (retaining about 82% and 71% of the sky respectively, Gold *et al.* 2009), there is little power over the angular range 60° - 160° . However, there is some non-zero correlation if the pixel estimator is evaluated over the full sky. Figure 1(b) shows the correlation functions determined from

[†] We used degraded resolution (NSIDE=16) versions of these masks. The degraded resolution KQ75 mask is plotted in Figure 4.

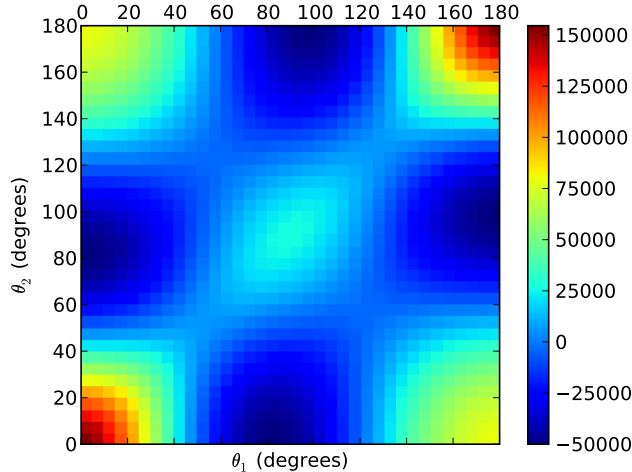


Figure 2. Covariance matrix for the pixel correlation estimator (3) computed for full sky maps. The scale on the right is in units of $(\mu\text{K})^4$.

the pseudo-spectra (5). This simply confirms the equivalence of the two estimators (3) and (5) (apart from minor differences arising from the finite angular bin widths). The covariance matrix for these estimators for the full sky is shown in Figure 2, using the C_ℓ for the six parameter ΛCDM model that provides the best fit to the WMAP data (Komatsu *et al.* 2009). The large angle ACF for a nearly scale invariant temperature spectrum is dominated by a small number of modes leading to large correlations between different angular scales. The main effect of a KQ75-type sky cut on the covariance matrix is to increase its overall amplitude. The angular structure of the covariance matrix is insensitive to the precise size and shape of the sky cut.

The results plotted in Figure 1 are very similar to those presented by S03 and E04 using a slightly different estimator

$$C^P(\theta) = \frac{1}{4\pi} \sum_{\ell} (2\ell + 1) \hat{C}_\ell^P P_\ell(\cos \theta), \quad \hat{C}_\ell^P = M_{\ell\ell'}^{-1} \tilde{C}_{\ell'}^P, \quad (12)$$

where the matrix M is

$$M_{\ell\ell'} = \frac{1}{(2\ell + 1)} \sum_{mm'} |K_{\ell m \ell' m'}|^2. \quad (13)$$

If we assume statistical isotropy, then both of the estimators (3) and (12) are unbiased estimators of the ensemble mean ACF and the power spectrum estimate \hat{C}_ℓ^P is an unbiased estimate of the true power spectrum $\langle C_\ell \rangle$. (The matrix \mathbf{M}^{-1} ‘deconvolves’ the PCL estimates \tilde{C}_ℓ^P correcting the bias introduced by a sky cut, Hivon *et al.* 2002).

One can see from (5) that the estimators (3) and (12) are identical for the complete sky, since then

$$w_{\ell m} = (2\pi)^{1/2} \delta_{\ell 0} \delta_{m 0}, \quad M_{\ell\ell'} = \delta_{\ell\ell'}. \quad (14)$$

The estimators (3) and (12) will, however, differ if a sky cut is applied to the data. Nevertheless, since both estimators involve sums over pseudo-spectral coefficients, and since they are formally identical for the full sky, one would expect that they would return similar estimates when applied to data incorporating moderate sky cuts such as the KQ85 and KQ75 masks.

This is, indeed, what we find. Figure 3 shows the estimator (12) applied to the WMAP 5 year ILC map. The results are almost identical to those shown in Figure 1. The pixel estimator of the ACF (3) is therefore almost identical to the estimator of (12) and so, as expected, it contains little new information (regardless of any assumptions concerning statistical isotropy).

The main differences between the various ACF estimates plotted in Figures 1 and 3 come from application of the sky cuts. With the sky cuts applied, the ACF’s are close to zero on angular scales $\gtrsim 60^\circ$. This lack of power leads to particularly low values for the $S_{1/2}$ statistic of about 1000-2000 $(\mu\text{K})^4$, as listed in Table 1. If no sky cut is applied, the value of the $S_{1/2}$ statistic is substantially higher at around 8000 $(\mu\text{K})^4$. It is worth noting that the values listed in Table 1 are very similar to the values obtained from the WMAP first year data (*cf* Table 5 in E04). The low multipole anisotropies that contribute to the ACF at large angular scales have remained stable as the data have improved. The low multipoles are signal dominated and stable to improved gain corrections, foreground separation and small perturbations to the Galactic mask.

As discussed in the Introduction, CHSS09 argue that the pixel estimates of the ACF computed from the masked regions of the sky lead to p-values with respect to the standard ΛCDM cosmology of $\sim 0.1\%$ or less, suggesting a significant discrepancy

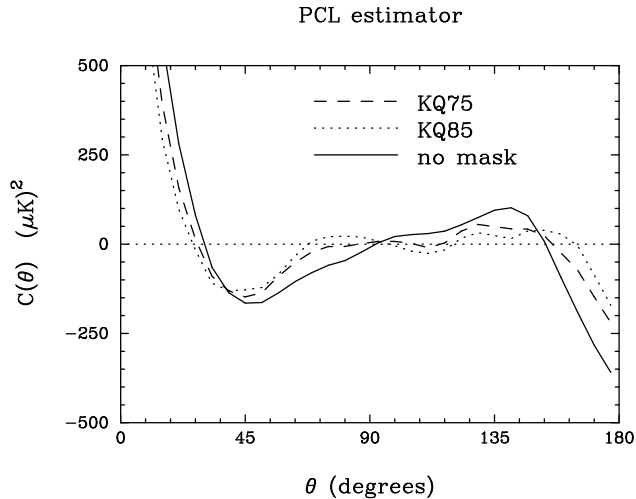


Figure 3. As in Figure 1 but using the pseudo-harmonic estimator of equation (12).

Table 1: Values of the $S_{1/2}$ statistic for WMAP 5 year ILC maps¹

sky cut	Pixel ACF (equ 3)	Pixel ACF (equ 5)	PCL ACF (equ 12)	$S_{1/2}$ statistic in $(\mu\text{K})^4$				QML ACF (equ 15)
				$\ell_{\max} = 5$	$\ell_{\max} = 10$	$\ell_{\max} = 15$	$\ell_{\max} = 20$	
full sky	7373	8532	8532	8170	7777	7649	7606	8532
KQ85	1401	1781	1901	8250	6953	7612	6383	7234
KQ75	647	963	1010	7913	6914	8233	5139	5764

¹ For maps degraded to Healpix resolution of NSIDE= 16 and smoothed with a Gaussian of FWHM 10° .

between the model and the data. However, the p-values computed for the unmasked sky are much less significant ($\sim 5\%$). Various interpretations of this result have been proposed:

(i) The interpretation put forward by CHSS09 is that either correlations have been introduced in reconstructing the full sky maps from the observations, or that there are highly significant departures from statistical isotropy that are correlated with the Galactic sky cut leading to an ACF that is very close to zero for regions outside the sky cut.

(ii) The interpretation put forward by E04 is that the low p-values are a consequence of using a sub-optimal estimator of the ACF on a cut sky, combined with a posteriori choices of the form of the $S_{1/2}$ statistic. On this interpretation, the low p-values found by S03, Copi *et al.* (2007) and CHSS09, are of no physical significance.

In support of point (ii), E04 used a quadratic maximum likelihood (QML) estimator of the power spectrum, \hat{C}_ℓ^Q , and computed the ACF

$$C^Q(\theta) = \frac{1}{4\pi} \sum_{\ell} (2\ell + 1) \hat{C}_\ell^Q P_\ell(\cos \theta). \quad (15)$$

For Gaussian temperature maps, the QML estimates \hat{C}_ℓ^Q have a significantly smaller variance than the PCL estimates \hat{C}_ℓ^P if a sky cut is applied to the data[‡]. Hence the estimator $C^Q(\theta)$ will generally be closer to the truth (*i.e.* closer to the ensemble mean $\langle C(\theta) \rangle$) than the estimator (12). Applied to the first year WMAP ILC map, E04 found that the ACF estimates derived from (15) are insensitive to a sky cut and lead to p-values for the S -statistic of $\sim 5\%$, *i.e.* no strong evidence against the concordance Λ CDM model.

The reason that the QML estimator has significantly smaller ‘estimator induced’ variance than the PCL estimator is easy to understand (see Efstathiou 2004b). For noise-free band limited data, it is possible to reconstruct the low multipole coefficients $a_{\ell m}$ exactly from data over an incomplete sky. This is, in effect, what the QML estimator does, though it implicitly assumes statistical isotropy in weighting the $a_{\ell m}$ coefficients to form the power-spectrum. For low multipoles, the assumption

[‡] For noise-free data over the full sky, the QML and PCL estimators are identical.

of statistical isotropy is unimportant, and for the noise-free data and sky cuts relevant to WMAP, the low order multipole coefficients and the power spectrum C_ℓ can be reconstructed almost exactly from data on the incomplete sky. In this paper, we will extend the analysis of E04 by explicitly reconstructing the low order coefficients $a_{\ell m}$ over the entire sky. This analysis will confirm that the ACF at large angular scales is insensitive to a sky cut and leads to p-values of marginal significance.

The ‘estimator induced’ variance of the pixel estimator of the ACF (3) is also easy to understand intuitively. (This problem has been discussed extensively in the literature in the context of angular clustering analysis of galaxy surveys: Groth and Peebles 1986; Landy and Szalay 1993; Hamilton 1993; Maddox, Efstathiou and Sutherland 1996). The ACF is a pair-weighted statistic. Consider the analysis of data on an incomplete sky. An overdensity, or underdensity, close to the boundary of the sky cut will almost certainly continue as an overdensity, or underdensity, across the cut. If the pair count is merely corrected by the missing area that lies within the cut region of sky (as in the estimator 3) overdense and underdense regions close to the boundary will be underweighted. This causes no bias to the estimator, but increases the sample variance. The analysis presented in the next Section shows that it is possible reduce this sampling variance by reconstructing the low multipoles across a sky cut in a way that is numerically stable and free of assumptions concerning statistical isotropy.

3 RECONSTRUCTING LOW-ORDER MULTIPOLES ON A CUT SKY

The aim of this Section is to reconstruct the large-scale features of the temperature anisotropies over the whole sky using only the incomplete data that lies outside a chosen sky cut. This can be done in a number of ways, for example, by Weiner or ‘power equalization’ filtering (Bielwicz, Górski and Banday, 2004), Gibbs sampling (Wandelt, Larson and Lakshminarayanan, 2004; Eriksen *et al.* 2004) or by ‘harmonic inpainting’ (Inoue, Cabella and Komatsu, 2008). Here we apply a direct inversion method, which is insensitive to assumptions concerning the statistical properties of the temperature field.

Let the vector \mathbf{x} denote the temperature field on the sky and let the vector \mathbf{a} denote the spherical harmonic coefficients $a_{\ell m}$. The vectors \mathbf{x} and \mathbf{a} are related by the spherical transform \mathbf{Y} ,

$$\mathbf{x} = \mathbf{Y}\mathbf{a} + \mathbf{n}, \quad (16)$$

where \mathbf{n} represents ‘noise’ in the data.

Now consider the reconstruction \mathbf{a}^e

$$\mathbf{a}^e = (\mathbf{Y}^T \mathbf{A} \mathbf{Y})^{-1} \mathbf{Y}^T \mathbf{A} \mathbf{x}, \quad (17)$$

for any arbitrary square matrix \mathbf{A} . The reconstruction is related to the true coefficients \mathbf{a} by

$$\mathbf{a}^e = \mathbf{a} + (\mathbf{Y}^T \mathbf{A} \mathbf{Y})^{-1} \mathbf{Y}^T \mathbf{A} \mathbf{n}. \quad (18)$$

If the data is noise free, (17) recovers the true vector \mathbf{a} exactly. If, further, we choose \mathbf{A} to be the identity matrix, then

$$\mathbf{a}^e = \mathbf{K}^{-1} \tilde{\mathbf{a}}, \quad (19)$$

where \mathbf{K} is the coupling matrix (9).

The reconstruction of (19) is closely related to the problem of defining an orthonormal basis set of functions on the cut sky, which has been studied extensively in the literature (see *e.g.* Górski 1994; Górski *et al.* 1994; Mortlock, Challinor and Hobson, 2002). If the sky cut is relatively small, and the data are noise-free and band-limited, the coupling matrix \mathbf{K} will be non-singular and can be inverted to yield the full-sky harmonics \mathbf{a} exactly. If the data are noise-free but not band-limited, the matrix \mathbf{K} will become numerically singular on the incomplete sky as $\ell_{\max} \rightarrow \infty$. (As a rule-of-thumb the matrix will become singular if ℓ_{\max} exceeds the inverse of the width of the sky cut in radians.) This simply tells us that there are ‘ambiguous’ harmonic coefficients that are unconstrained by the data outside the sky cut. For noise-free data that are not strictly band-limited, the solution (17) truncated to a finite value of ℓ_{\max} will amplify some of the high frequency signal which will appear as ‘noise’ within the sky cut in the reconstruction $\mathbf{x}^e = \mathbf{Y}\mathbf{a}^e$. The amplitude of this ‘noise’ can be reduced by an appropriate choice of the matrix \mathbf{A} . If we assume that the signal and noise are Gaussian, the optimal solution of (16) is the familiar ‘map-making’ solution

$$\mathbf{a}^e = (\mathbf{Y}^T \mathbf{C}^{-1} \mathbf{Y})^{-1} \mathbf{Y}^T \mathbf{C}^{-1} \mathbf{x}, \quad (20a)$$

$$\mathbf{C} = \langle \mathbf{x} \mathbf{x}^T \rangle = \mathbf{S} + \mathbf{N}, \quad (20b)$$

(de Oliveira-Costa and Tegmark 2006). If Gaussianity and statistical isotropy holds, the variance of the (20a) is

$$\langle \mathbf{a}^e \mathbf{a}^{eT} \rangle = \mathbf{C}_a = (\mathbf{Y}^T \mathbf{C}^{-1} \mathbf{Y})^{-1}. \quad (21)$$

The statement that the estimator (20a) is ‘optimal’ and the expression for the variance (21), do of course depend on the assumptions of Gaussianity and statistical isotropy. However, as long as the noise term in (18) is negligible, the reconstructed harmonic coefficients will be identical to the true harmonic coefficients *independent* of any assumptions concerning statistical isotropy.

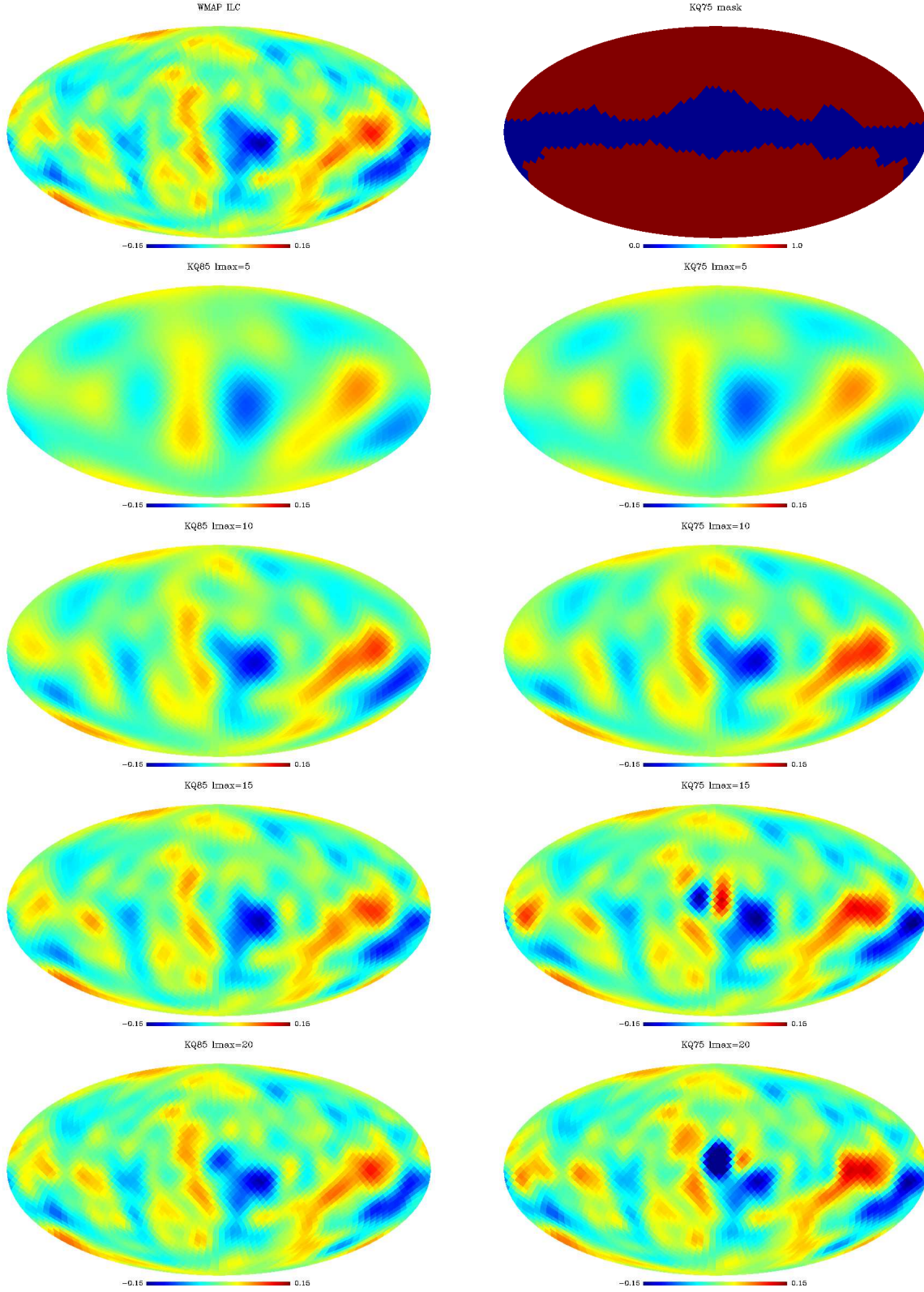


Figure 4. The figure to the left in the top row shows the WMAP 5 year ILC temperature map smoothed by a Gaussian of FWHM 10° and repixelized to a Healpix resolution of $\text{NSIDE}=16$. The figure to the right in the top panel shows the degraded resolution WMAP KQ75 mask used in this paper. The remaining figures to the left show the reconstructed all-sky maps computed from data outside the KQ85 sky cut, using the harmonic coefficients computed from equation (20a) with the coupling matrices truncated to (from top to bottom) $\ell_{\text{max}} = 5, 10, 15$ and 20 . The figures to the right show equivalent plots for the reconstructed all-sky maps computed from data outside the KQ75 sky cut.

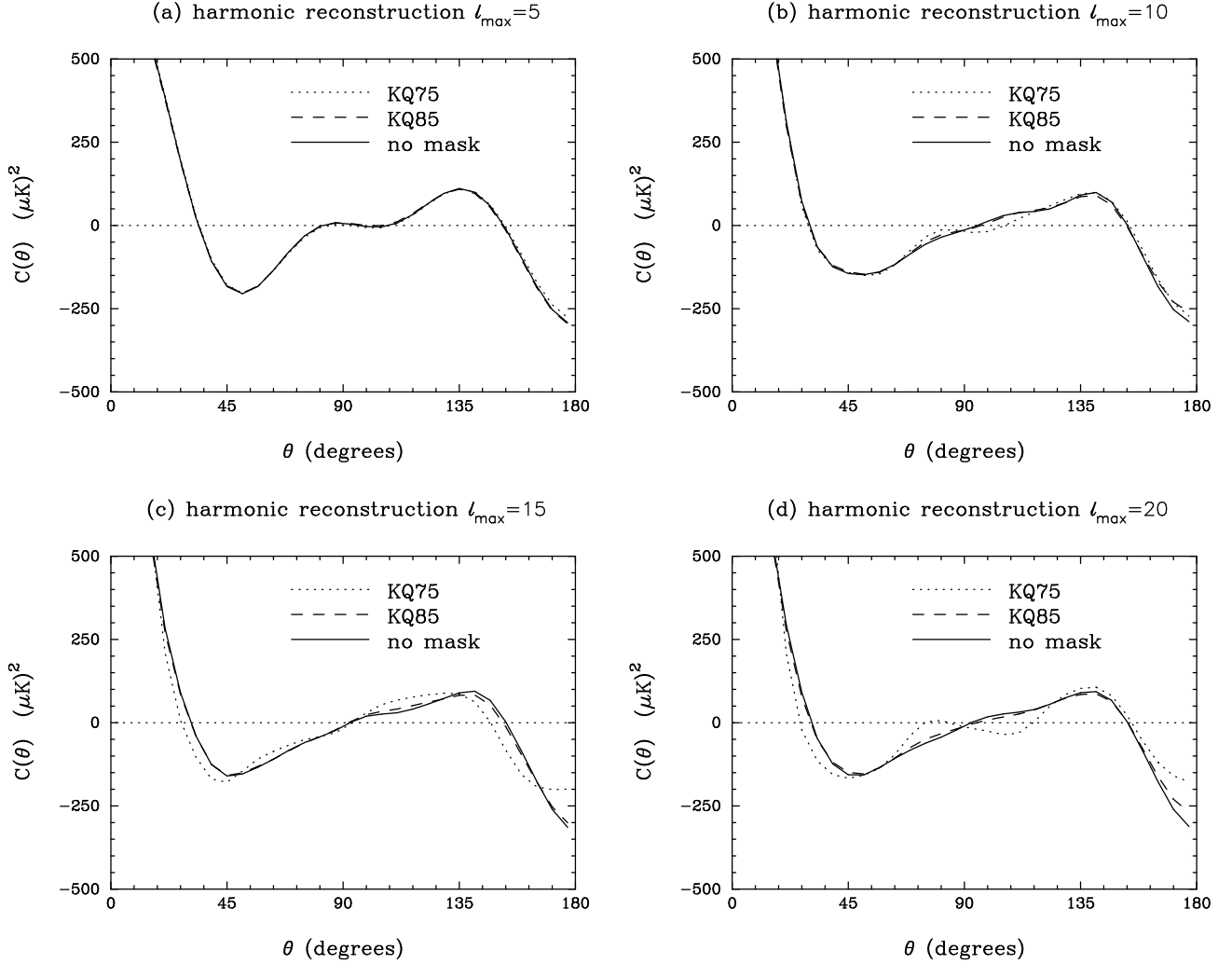


Figure 5. Reconstructions of the correlation function from equation (22) for various choices of ℓ_{\max} and sky cut.

Figure 4 illustrates the application of this machinery. The upper row shows the smoothed WMAP 5 year ILC map (to the left) and the degraded resolution KQ75 mask (to the right). The remaining figures show the reconstructed maps from the harmonic coefficients (20a) for the KQ85 mask (figures to the left) and for the KQ75 mask (figures to the right). The figures show the reconstructions with ℓ_{\max} truncated at 5, 10, 15 and 20. The maps for the two sky cuts at $\ell_{\max} = 5$ and 10 are virtually identical, and by $\ell = 10$ the reconstructions look visually similar to the ILC map over the entire sky. For $\ell_{\max} = 15$ and 20, the reconstructions for the KQ85 mask are stable and, again, look very similar to the WMAP ILC map over the whole sky. For the KQ75 mask, one can see ‘noise’ (*i.e.* reconstruction errors) beginning to appear inside the sky cut when ℓ_{\max} is increased to $\ell_{\max} = 15$ and 20,

However, the high harmonics that contribute to the ‘noise’ in Figure 4 make very little contribution to the correlation function at large angular scales. This is illustrated in Figure 5, which shows the dependence of the correlation functions

$$C^e(\theta) = \frac{1}{4\pi} \sum_{\ell=2}^{\ell_{\max}} (2\ell + 1) C_{\ell}^e P_{\ell}(\cos \theta), \quad C_{\ell}^e = \frac{1}{(2\ell + 1)} \sum_m |a_{\ell m}^e|^2, \quad (22)$$

on ℓ_{\max} for each of the each of the sky cuts. In the case of zero sky cut, the correlation function stabilises to its final shape by $\ell_{\max} = 10$; higher multipoles make a negligible contribution to the correlation function at large angular scales. The reconstructed correlation functions for the KQ85 and KQ75 masks are almost identical to the all-sky correlation function for $\ell_{\max} = 5, 10$ and 15. For the KQ75 mask, one can begin to see the effects of reconstruction noise in $C^e(\theta)$ for $\ell_{\max} = 20$, but the correlation function for the KQ85 mask remains stable.

This analysis shows that it is possible to reconstruct the low order harmonic coefficients that contribute to the large angle correlation functions accurately from data on the cut sky. The sky cut is basically irrelevant and so the all-sky form

of the correlation function can be reconstructed from the cut sky irrespective of any assumptions concerning Gaussianity or statistical isotropy. Values for the $S_{1/2}$ statistic for each of the cases shown in Figure 5 are listed in Table 1.

Notice that if we define weighted harmonic coefficients,

$$\boldsymbol{\beta} = \mathbf{C}_{\mathbf{a}}^{-1} \mathbf{a}^e = Y_{\ell m}^*(\boldsymbol{\theta}_i) C_{ij}^{-1} x_j, \quad (23)$$

then the power spectrum computed from these weighted coefficients is

$$y_\ell = \frac{1}{2} \sum_m |\beta_{\ell m}|^2 = x_p x_q E_{pq}^\ell, \quad (24)$$

where

$$\mathbf{E}^\ell = \frac{1}{2} \mathbf{C}^{-1} \frac{\partial \mathbf{C}}{\partial C_\ell} \mathbf{C}^{-1}. \quad (25)$$

In other words, the power spectrum of the weighted coefficients is identically equivalent to the QML power spectrum estimator (Tegmark 1997, de Oliveira-Costa and Tegmark 2006). If statistical isotropy holds, and the data is noise-free, the quantity

$$\hat{\mathbf{C}}^{\mathbf{Q}} = \mathbf{F}^{-1} \mathbf{y}, \quad (26)$$

provides an unbiased estimate of the power spectrum, where \mathbf{F} is the Fisher matrix,

$$F_{\ell\ell'} = \frac{1}{2} \text{Tr} \left[\mathbf{C}^{-1} \frac{\partial \mathbf{C}}{\partial C_\ell} \mathbf{C}^{-1} \frac{\partial \mathbf{C}}{\partial C_{\ell'}} \right]. \quad (27)$$

Notice that for the complete sky, and for noise-free data

$$\mathbf{C}_{\mathbf{a}} = C_\ell \delta_{\ell\ell'} \delta_{mm'}, \quad (28)$$

in the limit $\ell_{\max} \rightarrow \infty$, *i.e.* the variance on the $a_{\ell m}$ is just the cosmic variance. The Fisher matrix is

$$F_{\ell\ell'} = \frac{(2\ell + 1)}{2C_\ell^2} \delta_{\ell\ell'}, \quad (29)$$

and so the QML estimates $\hat{C}_\ell^{\mathbf{Q}}$ are identical to the PCL estimates. For relatively small sky cuts such as the KQ85 and KQ75 masks, the Fisher matrix at low multipoles will be *almost* diagonal (see Efstathiou 2004b) and the recovered power spectrum from the cut sky will be almost identical to the true power spectrum computed from the whole sky. The QML estimator effectively performs the reconstruction \mathbf{a}^e of equation (20a), but uses the assumption of statistical isotropy to downweight ‘ambiguous’ modes that are poorly constrained by the sky cut.

For small sky cuts, we would therefore expect the QML correlation function estimate (15) to be almost identical at large-angular scales to the correlation functions computed from the reconstructed coefficients \mathbf{a}^e . (They are, of course, mathematically identical for zero sky cut.) $C^{\mathbf{Q}}(\theta)$ is expected to behave more stably than $C^e(\theta)$ as the sky cut is increased, since the QML correlation function downweights ambiguous modes. This is exactly what we see when we apply the QML estimate to the WMAP ILC 5 year ILC maps (see Figure 6). The angular correlation function is almost independent of the sky cut, confirming the results of E04. Values of the $S_{1/2}$ statistic for the QML ACF estimates are listed in the final column of Table 1.

The QML power spectrum estimates are plotted in Figure 7. The power spectrum coefficients $\hat{C}_\ell^{\mathbf{Q}}$ are extremely stable to the sky cut, varying by only a few tens of $(\mu\text{K})^2$ for $\ell \leq 10$. The figure compares these estimates to the power spectrum estimates for the reconstructed all-sky maps using equation (20a). We plot the results for $\ell_{\max} = 10$, since this value is large enough to determine the shape of the ACF at large angular scales, but small enough to limit the noise in the reconstructed maps at high multipoles. The power spectra of the reconstructed maps are very close to the QML estimates at $\ell \leq 8$, though one can begin to see the effects of reconstruction noise in the KQ75 case at $\ell > 8$. (However, as Figure 5b shows, this reconstruction noise has very little effect on the shape of the ACF at large angular scales.)

The results of this section show that the low-order multipole coefficients that determine the behaviour of the correlation function at large angular scales can be reconstructed to high accuracy from data on the incomplete sky, independent of any assumptions concerning statistical isotropy. The usual motivation for applying a sky cut is to remove regions of the sky that may be contaminated by residual Galactic emission. However, for the KQ85 and KQ75 sky cuts, the missing area of sky leads to little loss of information at low multipoles. The low multipoles can therefore be reconstructed from the data on the incomplete sky. The imposition of the sky cuts does not remove foreground contamination at these low multipoles: any residual Galactic contribution to the low multipoles in the ILC map is, like the CMB signal, faithfully reproduced by the reconstructions shown in Figure 4. What a Galactic cut can do is to mask out localised Galactic emission (‘ambiguous’ modes) that could, in principal, couple to the low multipoles in a way that depends on the estimator (*e.g.* via the coupling matrix \mathbf{K} in the simple inversion of equation (19)). The similarities between the reconstructions of Figure 4 and the full-sky ILC map (and the correlation functions and power spectra plotted in Figures 5-7) show that the ILC map has removed Galactic

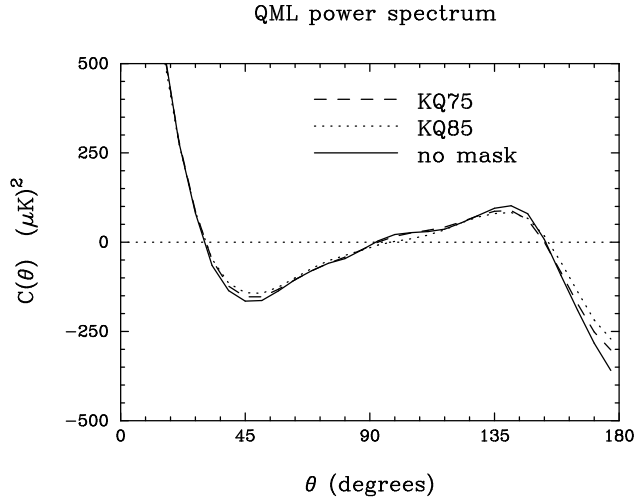


Figure 6. As Figure 1 but using the QML estimator of equation (15).

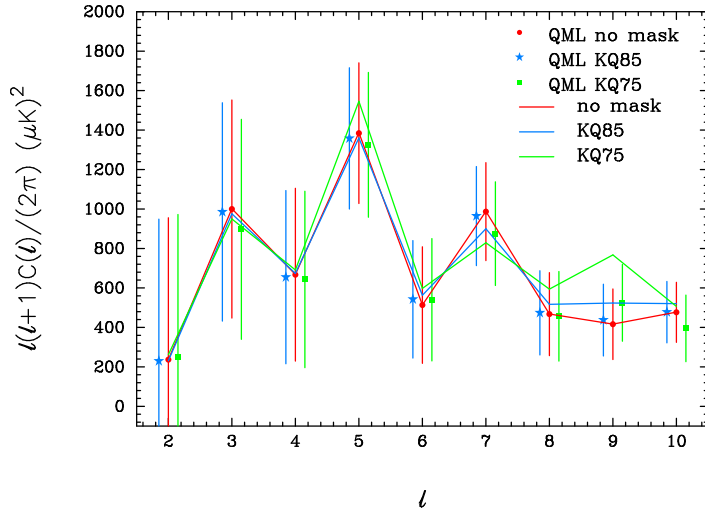


Figure 7. The temperature power spectrum at low multipoles computed from the low resolution WMAP 5 year ILC map. The points (corrected for the 10° FWHM smoothing and slightly displaced in l for clarity) show QML power spectrum estimates for three sky cuts: no mask; KQ85 mask; KQ75 mask. Error bars show the diagonal components of the inverse of the Fisher matrix (27). The solid red line shows the power spectrum computed from the all-sky ILC map (which is identical to the QML all-sky estimates). The solid green and blue lines show the power spectra computed for the $l_{\max} = 10$ reconstructions of Figure 4.

emission successfully at low Galactic latitudes, since there is no evidence of high amplitude ‘ambiguous’ modes in the ILC map within the region of the sky cut.

If suitable estimators are applied to noise-free data, a sky cut of the size of the KQ85 or KQ75 masks has little impact on the reconstruction of the low order multipoles or the all-sky ACF. The imposition of a sky cut does, however, lead to a loss of information if a poor estimator is used to estimate the ACF. This is what happens when the pixel estimator (3) is used to estimate the ACF on the cut sky (Copi *et al.* 2007; Hajian 2007; CHSS09). The analysis presented in this Section provides compelling evidence that the true value of the $S_{1/2}$ statistic for our realization of the sky is in the region of $6000\text{--}8000(\mu\text{K})^4$, independent of the sky cut.

4 ANALYSIS OF THE $S_{1/2}$ STATISTIC

In this Section we analyse the $S_{1/2}$ statistic, first from a Bayesian point of view, and then from a frequentist point of view. We then discuss the interpretation of the low frequentist p-values found by CHSS09.

4.1 Approximate Bayesian analysis

We begin by performing an approximate Bayesian analysis to compute the posterior distribution of the $S_{1/2}$ given the data on the assumption that the fluctuations are Gaussian and statistically isotropic. If the data were noise-free and covered the entire sky then, under the assumptions of statistical isotropy and Gaussianity, the data power spectrum C_ℓ^d provides a loss-free description of the data. Assuming uniform priors on each of the C_ℓ^T , the posterior distribution of the theory power spectrum coefficients C_ℓ^T is given by the inverse Gamma distribution

$$dP(C_\ell^T | C_\ell^d) \propto \left(\frac{C_\ell^d}{C_\ell^T} \right)^{\frac{2\ell-1}{2}} \exp \left[-\frac{(2\ell+1)}{2} \left(\frac{C_\ell^d}{C_\ell^T} \right) \right] \frac{1}{C_\ell^T}. \quad (30)$$

Each of the C_ℓ^T is statistically independent and the mean value is

$$\langle C_\ell^T \rangle = \left(\frac{2\ell+1}{2\ell-3} \right) C_\ell^d. \quad (31)$$

The distribution (30) will therefore favour theory values that are larger than the observed values C_ℓ^d .

The results of the previous Section (and Figure 7 in particular) show that the low multipoles are well determined and insensitive to the application of a sky cut. We can therefore use the measurements C_ℓ^d computed over the whole sky to represent the data[§]. The multipole expansion is truncated at $\ell_{\max} = 20$ (although as discussed in the previous Section, multipoles greater than $\ell \approx 10$ make very little contribution to the ACF at large angular scales) and statistically independent C_ℓ^T values are generated from the inverse Gamma distribution (30). These values are then used to generate Gaussian $a_{\ell m}^T$ from which we synthesize real-space maps x_i at a Healpix resolution of NSIDE=16 smoothed with a Gaussian of FWHM 10° . We then compute $S_{1/2}$ from the pixel correlation function (3). This methodology provides a test of statistically isotropic, Gaussian models, with no additional constraints imposed on the theory C_ℓ^T apart from uniform priors.

The posterior distributions of $S_{1/2}^T$ is shown in Figure 8a for the analysis of all-sky maps (red histogram) and for maps with the KQ75 mask applied (blue histogram). The distribution for the trials with the sky cut applied is slightly broader than the distribution for the all-sky trials, as expected since the pixel ACF estimator is sub-optimal on a cut sky. The peaks of the distributions occur at $S_{1/2}^T \approx 6000 (\mu\text{K})^4$ and so low values of $S_{1/2}^T$ are clearly preferred by the data. However, the posterior distributions have a very long tail to high values (as expected from the inverse Gamma distribution 30). The best fitting six parameter Λ CDM model as determined from the 5 year WMAP analysis (Komatsu *et al.* 2009) has a value of $S_{1/2}^T \sim 49000 (\mu\text{K})^4$. At this value (indicated by the vertical dashed line in Figure 8a), the posterior distribution has fallen to a value of about 0.4. Such high values of $S_{1/2}^T$ are evidently not favoured by the data, but they are not strongly disfavoured. Very low values of $S_{1/2}^T$, of $\sim 1000 (\mu\text{K})^4$ are also not strongly disfavoured.

From the Bayesian point of view, the quantity $S_{1/2}$ is a poor discriminator of theoretical models and so is relatively uninformative. The posterior distributions of Figure 8a are extremely broad with a long tail to high values. The data, irrespective of estimator or sky cut, clearly prefer low values of $S_{1/2}$ but cannot exclude the value of $S_{1/2}^T \sim 49000 (\mu\text{K})^4$ expected for the concordance inflationary Λ CDM model.

4.2 Frequentist analysis

We now generate statistically isotropic Gaussian realizations with the C_ℓ^T constrained to those of the best fitting Λ CDM model. The frequency distributions of $S_{1/2}$ computed from the pixel estimator are plotted in Figure 8b. The distributions of Figures 8a and 8b look fairly similar, but the frequentist interpretation is very different. For the all-sky analysis, the p-value of finding $S_{1/2} < 7373 (\mu\text{K})^4$ is 8% and hence is not statistically significant. However, if we apply the KQ75 mask, the p-value for $S_{1/2} < 647 (\mu\text{K})^4$ is only 0.065%. This result appears strongly significant and, at face value, inconsistent with the p-value for the all-sky analysis.

The low p-value found here and by S03 and CHSS09 come exclusively from analysing cut sky maps with ‘sub-optimal’ (in the sense of not reproducing the ACF for the whole sky) estimators. The sky cuts, ostensibly imposed to reduce any effects of Galactic emission at low Galactic latitudes, lead to a loss of information and to poorer estimates of the ACF for our realization of the sky. But as we have demonstrated, the information on the ACF at large angles for our realization of the sky is contained in the data outside the sky cuts. The imposition of a sky cut therefore has nothing to do with reducing the effects

[§] It is in this sense that the analysis presented here is described as an ‘approximate’, *i.e.* any residual errors on the C_ℓ^d are ignored.

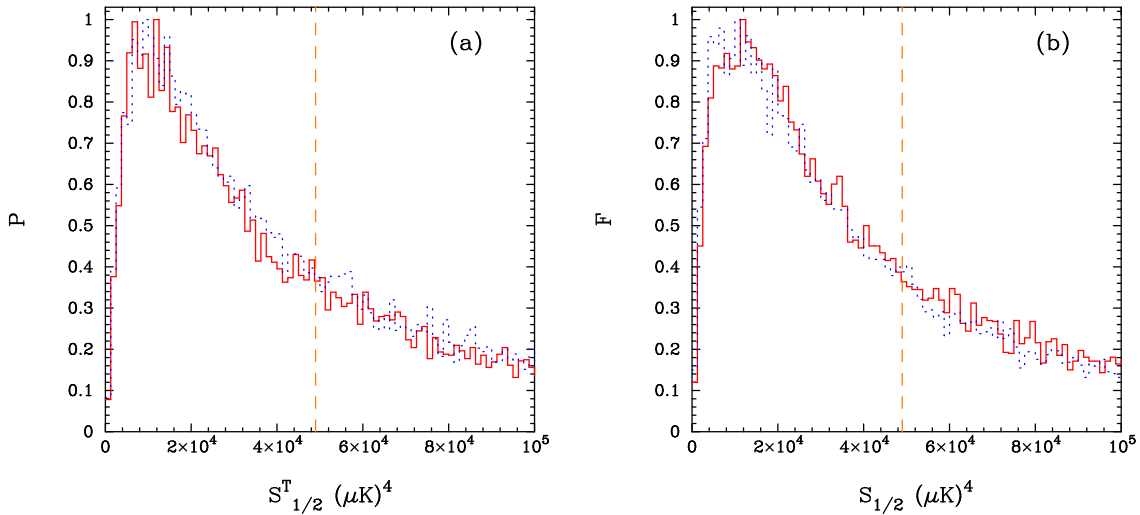


Figure 8. (a) Posterior distributions of $S_{1/2}^T$ computed as discussed in the text. The red (solid) histogram shows the distribution of $S_{1/2}^T$ from an analysis of the whole sky. The blue (dotted) histogram shows the distribution computed with the KQ75 sky cut applied. The vertical dashed lines in the figures shows the value $S_{1/2}^T \sim 49000 (\mu\text{K})^4$ for the best fitting ΛCDM model as determined from the 5 year WMAP analysis (Komatsu *et al.* 2009). (b) Frequency distributions of $S_{1/2}$ for statistically isotropic, Gaussian, realizations of the (Komatsu *et al.* 2009) ΛCDM model. The red (solid) histogram shows the frequency distribution for the pixel ACF estimator applied to the whole sky. The blue (dotted) histogram shows the distribution computed with the pixel ACF estimator with the KQ75 sky cut applied.

of Galactic emission on the ACF at large angular scales. If there is any cosmological significance to the low p-values, then one must accept that the Galactic cut aligns with the signal, *purely by coincidence*, in just such a way as to remove the large-scale angular correlations for particular choices of estimator of the ACF. This alignment may indicate a violation of statistical isotropy, as argued by CHSS09, but if this is true the alignment with the Galactic plane must be purely coincidental.

It seems to us that a more plausible interpretation of the low p-values is that they are a consequence of the *a posteriori* selection of the $S_{1/2}$ statistic by Spergel *et al.* (2003) for a particular choice of estimator and sky cut. It is difficult to quantify the effects of *a posteriori* choices. However, numerical tests with the more general statistic

$$S_\mu^p = \left[\frac{2}{3(1+\mu)} \int_{-1}^{\mu} [C(\theta)]^p d\cos\theta \right]^{2/p}, \quad (32)$$

(which reduces to $S_{1/2}$ for the choices $\mu = 1/2$ and $p = 2$) suggest that it is possible to alter p-values by an order of magnitude or more by selecting the parameters in response to the data. It would be possible to raise the p-values even more by varying the size and orientation of a sky cut.

Is there any way of testing this hypothesis further? In the ΛCDM model, the integrated Sachs-Wolfe (ISW) effect (Sachs and Wolfe, 1967) makes a significant contribution to the total temperature anisotropy signal at low multipoles. The ISW contribution from the time of last scattering (t_{LS}) and the present day (t_0) is given by

$$\frac{\Delta T}{T}^{\text{ISW}} = 2 \int_{t_{\text{LS}}}^{t_0} \frac{d\Phi}{dt} dt \quad (33)$$

where Φ is the Newtonian gravitational potential (see *e.g.* Mukhanov 2005). Recently, Francis and Peacock (2009) have used the 2MASS near infrared all-sky survey (Jarrett 2004), together with photometric redshift estimates to compute the ISW contribution from local structure at redshifts $z < 0.3$. If *a posteriori* choices are responsible for the low p-values, we should find large changes to the pixel ACF estimates for the masked sky when the WMAP ILC maps are corrected for the local ISW contribution. As shown in Figure 9, this is indeed what we find when we subtract the local ISW contribution computed by Francis and Peacock from the 5 year WMAP ILC map. The $S_{1/2}$ statistic computed from the ACFs shown in Figure 9 are $10360 (\mu\text{K})^4$ (all-sky), $6463 (\mu\text{K})^4$ (KQ85 mask) and $5257 (\mu\text{K})^4$ (KQ75 mask), all consistent with the concordance ΛCDM model at the few percent level. This is consistent with our hypothesis that the CHSS09 low p-values are a fluke, unless one is prepared to argue that there is a physical alignment of local structure with the potential fluctuations at the last scattering surface that conspires to remove large-angle temperature correlations in the regions outside the Galactic mask

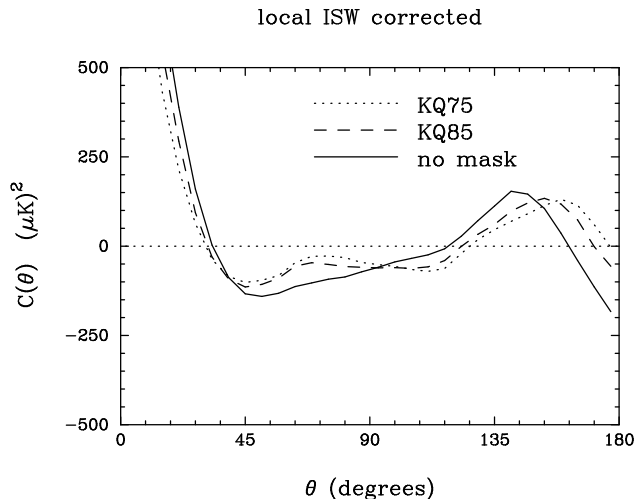


Figure 9. Pixel based estimates ACF estimates for the WMAP ICL map corrected for the local ISW contribution for redshift $z < 0.3$ as described by Francis and Peacock (2009).

(which seems implausible). Francis and Peacock (2009) discuss how the local ISW correction affects a number of other low multipole statistics, in particular reducing the statistical significance of the alignment between the quadrupole and octopole.

5 DISCUSSION AND CONCLUSIONS

The low amplitude of the temperature autocorrelation function at large angular scales has led to some controversy since the publication of the first year results from WMAP. This paper has sought to clarify the following points:

[1] We have compared different estimators of the ACF showing: (a) how they depend on assumptions of statistical isotropy; (b) how they are interrelated; (c) how they perform on the WMAP 5 year ILC maps with and without a sky cut.

[2] The imposition of the KQ85 and KQ75 sky masks leads to little loss of information on the low multipoles that contribute to the large-scale angular correlation function. As demonstrated in Section 3, the low multipole harmonics can be reconstructed accurately, independent of any assumptions concerning statistical isotropy, from the data that lie outside the sky cuts. The ACFs computed from these reconstructions are in good agreement with the ACF computed from the whole sky and in good agreement with the maximum likelihood estimator (15). There can be little doubt that the large-scale ACF for our realization of the sky is very close to the all-sky results shown in Figures 1, 3 and 6, independent of any assumptions regarding statistical isotropy.

[3] The Bayesian analysis presented in Section 4 shows that the posterior distribution of the $S_{1/2}^T$ is broad and cannot exclude the value $S_{1/2}^T \sim 49000 (\mu\text{K})^4$ appropriate for the Komatsu *et al.* (2009) best fitting inflationary Λ CDM model. The breadth of the posterior distribution $S_{1/2}^T$ distribution shows that it is fairly uninformative statistic and so is not a particularly good discriminator of theoretical models.

[4] Unusually low values of the $S_{1/2}$ statistic are found only if ‘sub-optimal’ ACF estimators are applied to maps that include a Galactic mask. We have argued that the low p -values associated with these low values of $S_{1/2}$ are most plausibly a result of *a posteriori* choices of statistic. This seems plausible because: (a) S -type statistics are relatively uninformative and hence sensitive to *a posteriori* choices; (b) the all-sky ACF (which is compatible with the concordance Λ CDM model) can be recovered from the data outside the mask and so any physical model for the low p -values requires a fortuitous alignment of the temperature field with the Galaxy; (b) the analysis of the local ISW corrected maps presented in Section 4 suggests that any physical model of the low p -values requires a precise alignment of local structure with the large-scale potential fluctuations at the last scattering surface.

In summary, the results of this paper suggest that, irrespective of the imposition of Galactic sky cuts or assumptions of statistical isotropy, the large-scale correlations of the CMB temperature field provide unconvincing evidence against the concordance inflationary Λ CDM cosmology.

Acknowledgments: The authors acknowledge use of the Healpix package and the Legacy Archive for Microwave Background Data Analysis (LAMBDA). Support for LAMBDA is provided by the NASA Office of Space Science. We are particular grateful

to John Peacock and Caroline Francis for allowing us to use their ISW maps. Yin-Zhe Ma thanks Trinity College Cambridge and Cambridge Overseas Trusts for support. Duncan Hanson is grateful for the support of a Gates scholarship.

REFERENCES

- Basak S., Hajian A., Souradeep T., 2006, PRD, 74, 021301.
- Bennett C.L. *et al.*, 2003, ApJS, 148, 1.
- Bielwicz P., Górski K.M., Banday A.J., 2004, MNRAS, 355, 1283.
- Copi C.J., Huterer D., Schwarz D.J., Starkman G.D., 2009, MNRAS, in press. (CHSS09)
- Copi C.J., Huterer D., Schwarz D.J., Starkman G.D., 2007, PRD, 75, 3507.
- de Oliveira-Costa A., Tegmark M., Zaldarriaga M., Hamilton A., 2004, PRD, 69, 063516.
- de Oliveira-Costa A., Tegmark M., 2006, PRD, 74, 023005.
- Efstathiou G., 2004a, MNRAS, 348, 885. (E04)
- Efstathiou G., 2004b, MNRAS, 349, 603.
- Eriksen H.K., O'Dwyer I.J., Jewell J.B., Wandelt B.D., Larson D.L., Górski K.M., Levin S., Banday A.J., Lilje P.B., 2004, ApJS, 155, 227.
- Francis C.L., Peacock, J.A., arXiv:astro-ph/0909.2495.
- Gold B. *et al.*, 2009, ApJS, 180, 265.
- Górski K., 1994, ApJ, 430, L85.
- Górski K., Hinshaw G., Banday A.J., Bennett C.L., Wright E.L., Kogut A., Smoot G.F., Lubin P., 1994, ApJ, 430, L89.
- Górski K.M., Hivon E., Banday A.J., Wandelt B.D., Hansen F.K., Reinecke M., Bartlemann M., 2005, ApJ, 622, 759.
- Groth E.J., Peebles P.J.E., 1986, ApJ, 310, 499.
- Hajian A., 2007, arXiv:astro-ph/0702723.
- Hamilton A., 1993, ApJ, 417, 19.
- Hinshaw G., Banday A.J., Bennett C.L., Górski K.M., Kogut A., Smoot G.F., Wright E.L., 1996, ApJ, 464, L25.
- Hinshaw G. *et al.*, 2003, ApJS, 148, 135.
- Hinshaw G. *et al.*, 2009, ApJS, 180, 225.
- Hivon E., Górski K.M., Netterfield C.B., Crill B.P., Prunet S., Hansen F., 2002, ApJ, 567, 2.
- Inoue K.T., Cabella P., Komatsu E., 2008, PRD, 77, 123539.
- Jarrett T., 2004, Publications of the Astronomical Society of Australia, 21, 396.
- Komatsu E. *et al.*, 2009, ApJS, 180, 330.
- Land K., Magueijo J., 2005a, PRL, 95, 1301.
- Land K., Magueijo J., 2005b, MNRAS, 362, 838.
- Mortlock D.J., Challinor A.D., Hobson M.P., 2002, MNRAS, 330, 405.
- Landy S.D., Szalay A., 1993, ApJ, 412, 64L.
- Maddox S.J., Efstathiou G., Sutherland W.J., 1996, MNRAS, 283, 1227.
- Mortlock D.J., Challinor A.D., Hobson M.P., 2002, MNRAS, 330, 405.
- Mukhanov V., 2005, *Physical Foundations of Cosmology*, Cambridge University Press..
- Sachs R.K., Wolfe A.M., 1967, ApJ, 147, 73.
- Smoot G.F. *et al.*, 1992, ApJ, 396, L1.
- Spergel D.N. *et al.*, 2003, ApJ, 148, 175.
- Schwarz D.J., Starkman G.D., Huterer D., Copi C.J., 2004, PRL, 93, 1301.
- Tegmark M. 1997, PRD, 55, 5985.
- Tegmark M., de Oliveira-Costa A., Hamilton A.J., 2003, PRD, 68, 13523.
- Wright E.L. *et al.*, 1992, ApJ, 396, L13.
- Wandelt B.D., Larson D.L., Lakshminarayanan A., 2004, PRD, 70, 3511.